Available online at www.sciencedirect.com
ScienceDirect
Ceramics International 38 (2012) 847–850
CERAMICS INTERNATIONAL
www.elsevier.com/locate/ceramint

Short communication

Optical and morphological properties of Ce-doped TiO_2–MoO_3 ceramic matrix

S. Silvestri [a,*], E.T. Kubaski [b], R.A.P. Ribeiro [a], S.R. de Lazaro [a], S.A. Pianaro [a], S.M. Tebcherani [a]

[a] State University of Ponta Grossa, Av. Gal. Carlos Cavalcanti 4748, 84030-900 Ponta Grossa, PR, Brazil
[b] Itajara Minérios Ltda, Rua Balduíno Taques 650, 84010-050 Ponta Grossa, PR, Brazil

Received 19 November 2010; received in revised form 30 April 2011; accepted 26 May 2011
Available online 1st July 2011

Abstract

This study involves the production of a yellow ceramic pigment and examines the influence of the addition of Ce_2O_3 to a TiO_2–MoO_3 matrix processed by solid state reactions in a calcination step at 1200 °C. The presence of Ce^{+3} ions in the matrix leads to a decrease in the band gap value, intensifying the yellow color of the pigment. The absorbance spectra show light absorption in the visible region at a wavelength in the range of yellow color. The system under study results in a yellow pigment with a more intense color than that of the matrix.
© 2011 Elsevier Ltd and Techna Group S.r.l. All rights reserved.

Keywords: A. Powders-solid state reaction; C. Color; D. TiO_2; Pigments

1. Introduction

Ceramic pigment production requirements today include low product toxicity, cost reduction, and improved color shading, i.e., light and strong color intensity, using lower firing temperatures, due to the highly competitive market and the development of new materials [1]. These pigments are used for coloring materials such as glazes, paints and plastics [2].

The industrial ceramic pigments most widely employed are constituted of transition elements, which are characterized for having incomplete d or f orbitals, enabling the action of two phenomena responsible for pigmentation: electronic transitions within d–d or f–f levels, and charge transfer [3].

A pigment has a defined crystalline structure, which is determined by its host lattice [4]. At high temperatures, some oxides in a host lattice form either a solid solution or a new compound [5]. The majority of pigments composed of mixtures of transition-metal oxides show equilibrium between the metallic cations and the oxygen anions whose crystalline structure is similar to that of natural minerals [6].

TiO_2-based pigments are widely employed in industrial applications due to their color range, which depends on the chromophore ions [4,7] or counterions [8–10] added to the matrix. These pigments can also act as opacifying agents [6]. When Cr_2O_3 is added to TiO_2, whose structures are cassiterite and rutile, respectively, the mixture becomes yellow at 700 °C, and pink at 1400 °C [11]. The addition of ceria to the TiO_2 matrix results in a yellow pigment that can be employed in the fabrication of dental prostheses [12], with the possibility of obtaining a color similar to that of commercial dentine [12,13]. The doping of titanium oxide with vanadium and zirconium oxides produces a bright yellow shade whose colorimetric parameters are very similar to those of industrial ceramic pigments [14].

The addition of cerium and praseodymium to the TiO_2 matrix results in a color varying from yellow to red after calcination at 1250 °C; this pigment is employed as a plastic colorant [1,9]. In addition, the combination of cerium and molybdenum oxides yields a new environmentally friendly class of yellow pigments, thus serving as an alternative to toxic elements such as lead, cadmium and chromium [15].

Pigments containing molybdenum show different shades that change according to the matrix and temperature. For example, the addition of molybdenum to Al_2O_3 leads to a blue pigment [16].

The addition of dopants in oxide mixtures may change the pigment's color through band gap manipulation [1]. In other words, the use of dopants may shift the band gap energy to

* Corresponding author. Tel.: +55 42 3220 3053; fax: +55 42 3220 3160.
E-mail address: siarasilvestri@hotmail.com (S. Silvestri).

0272-8842/$36.00 © 2011 Elsevier Ltd and Techna Group S.r.l. All rights reserved.
doi:10.1016/j.ceramint.2011.05.161

values nearer to that necessary to obtain the desired color. For example, by doping $TiCeO_4$ with Pr^{+4} ions it is possible to obtain a reduction in the band gap from 2.96 to 1.84 eV; this decrease in the band gap causes the color to change. This first band gap value falls within the indigo region in the visible wavelength, leading to a light yellow color, while the second band gap value leads to a red brick color [1].

As mentioned earlier, pigments based on TiO_2 with a rutile structure are widely reported in the literature [17–19]. However, the synthesis of these pigments generally involves an anatase-to-rutile transformation, which is strongly affected by chromophores [17–19]. On the other hand, the crystal structure of rutile pigments, and, therefore their color properties, are modified by chromophore and counterion doping [17].

The present study involved the evaluation of a pigment with a new composition based on the rutile structure. This pigment was synthesized starting from rutile TiO_2 powders without involving the anatase-to-rutile transformation. The effect of the addition of Ce_2O_3 in increasing the yellow color intensity and lightness when compared with the TiO_2–MoO_3 matrix was also evaluated using the CIELab color system [4], as was the system's morphology.

2. Material and methods

The pigment was developed using a stoichiometric mixture of commercial titanium dioxide TiO_2 (Synth, 91%) and 20% (mole percentage) of molybdenum oxide (Vetec, 99%) as the matrix, and adding 0.1–1% (mole percentage) of $Ce(NO_3)_3{\cdot}6H_2O$ (Aldrich, 99.9%). The powder's particle sizes were 114 nm for titanium and 1.4 μm for molybdenum oxide.

The mixture was ground in an agate mortar and then calcined in a muffle furnace up to a final temperature of 1200 °C. For comparison with the doped samples, pure rutile TiO_2 samples were also sintered at 1200 °C. The furnace heating rate was 10 °C/min, and all the samples were sintered in air.

Samples of pure rutile TiO_2, MoO_3-doped TiO_2, and MoO_3–TiO_2 doped with 1% of $Ce(NO_3)_3{\cdot}6H_2O$ were characterized by X-ray diffraction (XRD) using a Shimadzu XRD6000 with CuKα radiation, with the patterns recorded from 10° to 70° in steps of 2°/min.

The particle size of the pigment was analyzed using a CILAS 920 particle size analyzer. The powder morphology was examined by scanning electron microscopy, using a Zeiss Supra 35 FEG-SEM microscope. The pigment's reflective capacity was characterized by UV-visible diffuse reflectance spectroscopy (360–830 nm), using a Varian Cary 50 spectrophotometer. The color of the samples was measured according to the ASTM D 2244-09b: Standard Practice for Calculation of Color Tolerances and Color Differences from Instrumentally Measured Color Coordinates, using the CIELab testing method.

The preparation of samples for UV-visible diffuse reflectance spectroscopy measurements consisted of grinding in an agate mortar and then sifting the material through a # 325 mesh laboratory test sieve.

The results of the UV-visible diffuse reflectance spectroscopy experiments were used to calculate the pigment band gap with the Kubelka–Munk function (K–M) [20], which is given by Eq. (1)

$$K - M = \frac{(1-R)^2}{2R} \tag{1}$$

where R is the reflectance.

The band gap is calculated using the reflectance as a function of wavelength curves, which are obtained by UV-visible diffuse reflectance spectroscopy. The reflectance curve is then extrapolated in the direction of the wavelength axis. This wavelength is the band gap wavelength, in nanometers, which is converted into energy (in electron volts) using Eq. (2)

$$E = \frac{1240}{\lambda} \tag{2}$$

where E is the band gap energy (eV) and λ is the wavelength (nm).

3. Results and discussion

The synthesized pigments were characterized by X-ray diffraction, and their patterns are shown in Fig. 1.

Fig. 1 presents the XRD pattern of pure TiO_2 (c) indicating the reflection of rutile crystalline phase. Fig. 1(b) shows the MoO_3 added to TiO_2, highlighting the three most intense reflections of MoO_3, as well as changes in the relative intensity of TiO_2 reflections. A sample powder system containing TiO_2, MoO_3, and Ce_2O_3 is shown in Fig. 1 (a).

A comparison of a calcined sample of the TiO_2–MoO_3 system containing 1% of Ce_2O_3 (Fig. 2(a)) and a non-calcined sample (Fig. 2(b)) shows changes in the XRD reflections, indicating that the introduction of cerium into the system contributed to promote structural changes in the rutile matrix. It can therefore be inferred that the structural changes in the matrix are due to a charge-transfer transition between Ti^{+4} ions and f electrons of Ce^{+3} or the conduction or valence ions of TiO_2.

Fig. 3 depicts the morphology of the TiO_2–MoO_3 system with and without Ce_2O_3 evaluated by SEM. These SEM micrographs suggest that the two samples had a similar

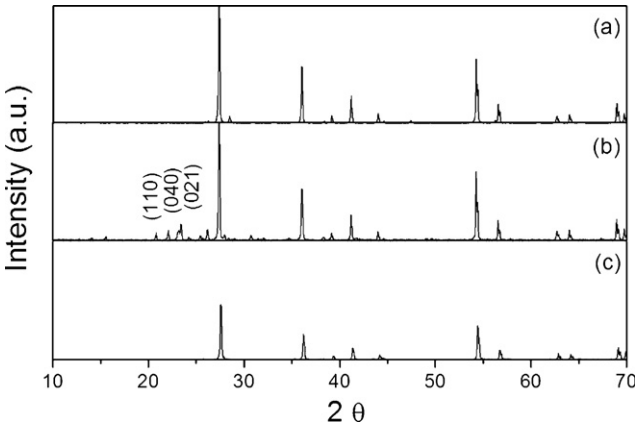

Fig. 1. XRD patterns of samples calcined at 1200 °C. (a) TiO_2–MoO_3 + Ce_2O_3, (b) TiO_2-MoO_3 (c) TiO_2.

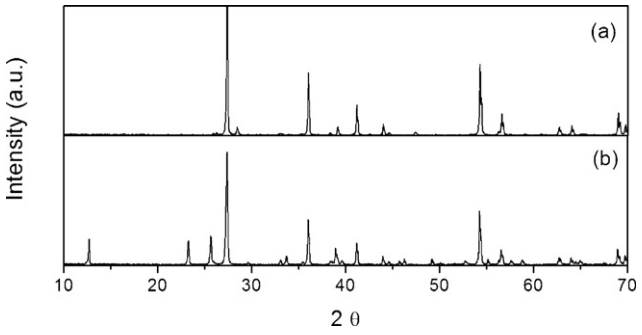

Fig. 2. XRD patterns of the TiO_2–MoO_3 system doped with 1% of Ce_2O_3: (a) calcined at 1200 °C; (b) non-calcined.

morphology, and that the calcination temperature employed sufficed to initiate the particle sintering process. The particle size analysis indicated that the pigment had a mean particle size of about 6.6 μm.

The absorbance of TiO_2–MoO_3 samples with different amounts of Ce_2O_3 was analyzed by UV-visible reflectance spectroscopy. The TiO_2–MoO_3 system was doped with 0.3, 0.5, 0.7, 0.9 and 1% (mole percentage) of Ce_2O_3. Absorbance spectra of the TiO_2–MoO_3 system without Ce_2O_3 and doped with 0.3 and 1% of Ce_2O_3 are shown in Fig. 4. The values of 0.3 and 1% of Ce_2O_3 represent, respectively, the maximum and minimum absorbance verified in the system under investigation. A comparison of Fig. 4(a)–(c) suggests only a small difference in absorption in the system containing Ce_2O_3, since the absorbance values fell within a narrow range.

The CIELab system includes three parameters for identifying a color [21]: the L^* parameter indicates the lightness level, which varies from 0 (black) to 100 (white); the a^* parameter: $a^* < 0$ indicates the amount of green while $a^* > 0$ indicates the amount of red; the b^* parameter: $b^* < 0$ indicates the amount of blue while $b^* > 0$ indicates the amount of yellow. Parameters a^* and b^* are the chromatic coordinates [14,22].

Fig. 5 shows the color parameters of the TiO_2–MoO_3 samples doped in the range of 0.0–1.0% of Ce_2O_3 estimated by the CiELab method. In comparison to the samples without Ce_2O_3, the increase in the amount of Ce_2O_3 did not promote an increase in lightness, as indicated by the L^* coordinate of the CIELab method.

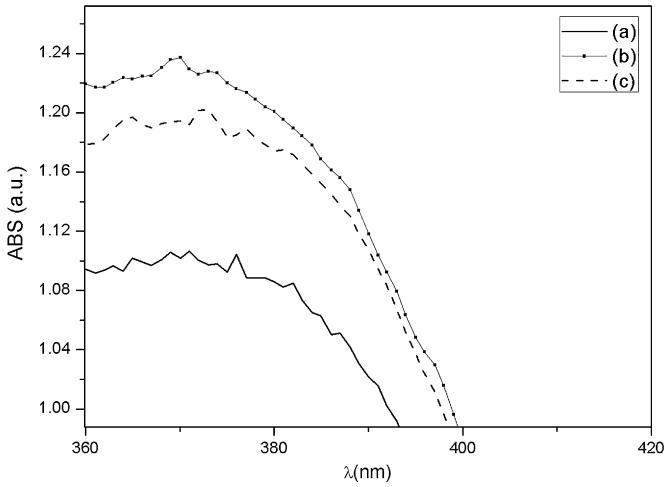

Fig. 4. Absorbance spectra of the TiO_2–MoO_3 system: (a) 0.0% Ce_2O_3; (b) 0.3% Ce_2O_3; and (c) 1.0% Ce_2O_3.

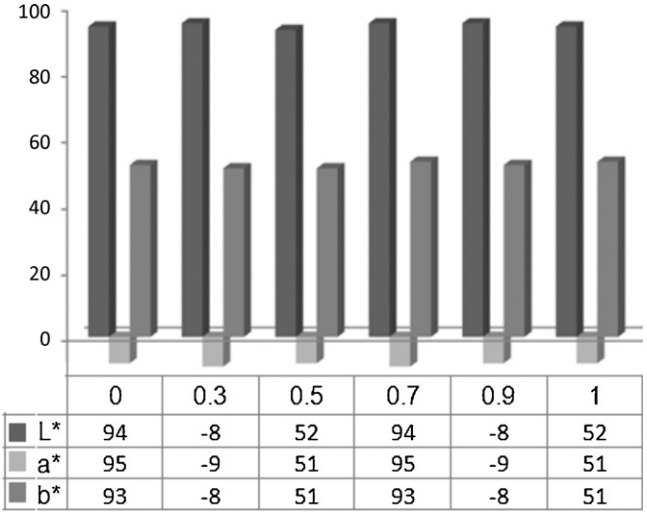

	0	0.3	0.5	0.7	0.9	1
L*	94	-8	52	94	-8	52
a*	95	-9	51	95	-9	51
b*	93	-8	51	93	-8	51

Fig. 5. L^*, a^* and b^* coordinates for the Ce_2O_3-doped TiO_2–MoO_3 system 0, 0.3, 0.5, 0.7, 0.9 and 1% in mol of Ce_2O_3.

According to the CiELab method coordinates, $-a^*$ indicates the maximum green intensity, and $+a^*$ the maximum red intensity. On the other hand, $-b^*$ indicates the maximum blue intensity, and $+b^*$ the maximum yellow intensity. Although it

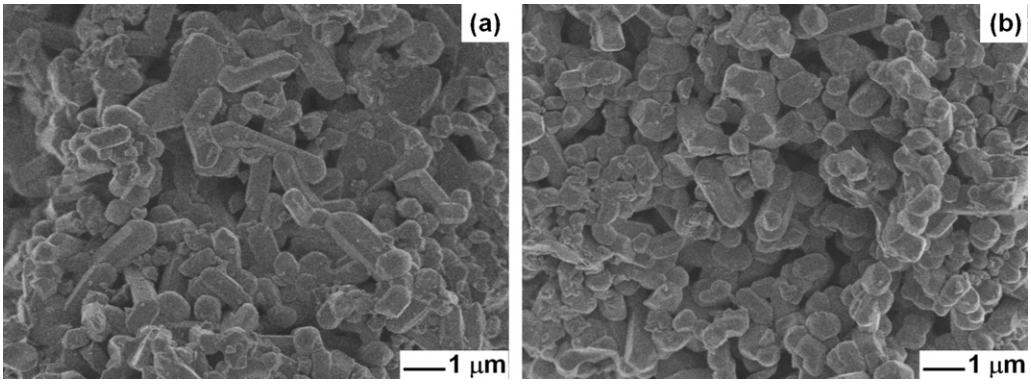

Fig. 3. SEM micrographs of the TiO_2–MoO_3 system calcined at 1200 °C: (a) TiO_2–MoO_3; (b) TiO_2–MoO_3 + Ce_2O_3.

Table 1
Gap values of pure the TiO_2–MoO_3 system, and the Ce_2O_3-doped system.

System	Gap (eV)
TiO_2–MoO_3	3.02
TiO_2–MoO_3 + 0.3% Ce_2O_3	3.02
TiO_2–MoO_3 + 1% Ce_2O_3	2.93

cannot be seen in Fig. 5, the addition of Ce_2O_3 to the TiO_2–MoO_3 matrix increases the intensity of yellow (+b*). This phenomenon may be due to the presence of Ce^{+3} ions, which promote yellow color added to a matrix.

The band gap was calculated using the Kubelka–Munk function (Eq. (1)) [20]. The band gap value indicates the minimum energy required to excite an electron. When the electron returns to its fundamental state, visible radiation is emitted at a wavelength in the range of 360–400 nm, which is the range absorbed by the pigment (Table 1).

Yellow is defined by a specific gap range, and the smaller the gap the lower the energy required to produce the color. The addition of Ce_2O_3 to the TiO_2–MoO_3 system decreases the gap value.

Colors depend on the number of unpaired electrons. Pigments derived from rare earths show their characteristic colors due to their intense charge-transfer interactions between a donor and a receptor, with the ion generally acting as a receptor.

As a result of the color obtained, the use of cerium as a doping agent in a system comprising a mixture of oxides promotes energy faults and displacement of electrons in conduction and valence bands.

4. Conclusions

The addition of Ce_2O_3 to the TiO_2–MoO_3 system up to a specific concentration limit enhances the intensity of the yellow color. This effect is produced by Ce_2O_3, whose presence diminishes the energy (gap) required to promote the yellow color.

Acknowledgments

The authors acknowledge the Brazilian research funding agencies CAPES, CNPq, and FINEP for their financial support.

References

[1] L.S. Kumari, G. George, P.P. Rao, M.L.P. Reddy, The synthesis and characterization of environmentally benign praseodymium-doped $TiCeO_4$ pigments, Dyes Pigments 77 (2) (2008) 427–431.
[2] P. Sulcová, M. Trojan, Study of $Ce_{1-x}Pr_xO_2$ pigments, Thermochim. Acta 395 (1–2) (2002) 251–255.
[3] Y. Marinova, J.M. Hohemberger, E. Cordoncillo, P. Escribano, J.B. Carda, Study of solid solutions, with perovskite structure, for application in the field of the ceramic pigments, J. Eur. Ceram. Soc. 23 (2) (2003) 213–220.
[4] P.M.T. Cavalcante, M. Dondi, G. Guarini, M. Raimondo, G. Baldi, Colour performance of ceramic nano-pigments, Dyes Pigments 80 (2) (2009) 226–232.
[5] D. Cordischi, D. Gazzoli, M. Occhiuzzi, M. Valigi, Redox behavior of VI B transition metal ions in rutile TiO_2 solid solutions: an XRD and EPR study, J. Solid State Chem. 152 (2) (2000) 412–420.
[6] V. Stengl, S. Bakardjieva, N. Murafa, Preparation and photocatalytic activity of rare earth doped TiO_2 nanoparticles, Mater. Chem. Phys. 114 (1) (2009) 217–226.
[7] F. Matteucci, G. Cruciani, M. Dondi, G. Gasparotto, D.M. Tobaldi, Crystal structure, optical properties and colouring performance of karrooite $MgTi_2O_5$ ceramic pigments, J. Solid State Chem. 180 (11) (2007) 3196–3210.
[8] V.S. Vishnu, G. George, V. Divya, M.L.P. Reddy, Synthesis and characterization of new environmentally benign tantalum-doped $Ce_{0.8}Zr_{0.2}O_2$ yellow pigments: applications in coloring of plastics, Dyes Pigments 82 (1) (2009) 53–57.
[9] P. Prabhakar Rao, M.L.P. Reddy, $(TiO_2)_1$ $(CeO_2)_{1-x}$ $(RE_2O_3)_x$ - novel environmental secure pigments, Dyes Pigments 73 (3) (2007) 292–297.
[10] M. Coster, X. Arnould, J.L. Chermant, L. Chermant, T. Chartier, The use of image analysis for sintering investigations: the example of CeO_2 doped with TiO_2, J. Eur. Ceram. Soc. 25 (15) (2005) 3427–3435.
[11] M.A. Tena, S. Meseguer, C. Gargori, A. Forés, J.A. Badenes, G. Monrós, Study of Cr–SnO_2 ceramic pigment and of Ti/Sn ratio on formation and coloration of these materials, J. Eur. Ceram. Soc. 27 (1) (2007) 215–221.
[12] S.F. Santos, M.C. de Andrade, J.A. Sampaio, A.B. da Luz, T. Ogasawara, Synthesis of ceria–praseodymia pigments by citrate-gel method for dental restorations, Dyes Pigments 75 (3) (2007) 574–579.
[13] M.-L. Brandily-Anne, J. Lumeau, L. Glebova, L.B. Glebov, Specific absorption spectra of cerium in multicomponent silicate glasses, J. Non-Cryst. Solids 356 (44–49) (2010) 2337–2343.
[14] M. Dondi, F. Matteucci, I. Zama, G. Cruciani, High-performance yellow ceramic pigments $Zr(Ti_{1-x-y}Sn_{x-y}V_yM_y)O4$ (M = Al, In, Y): crystal structure, colouring mechanism and technological properties, Mater. Res. Bull. 42 (1) (2007) 64–76.
[15] K.J. Sreeram, R. Srinivasan, J. Meena Devi, B. Unni Nair, T. Ramasami, Cerium molybdenum oxides for environmentally benign pigments, Dyes Pigments 75 (3) (2007) 687–692.
[16] S. Braun, L.G. Appel, V.L. Camorim, M. Schmal, Thermal spreading of MoO_3 onto silica supports, J. Phys. Chem. B 104 (28) (2000) 6584–6590.
[17] F. Matteucci, G. Cruciani, M. Dondi, M. Raimondo, The role of counterions (Mo, Nb, Sb, W) in Cr-, Mn-, Ni- and V-doped rutile ceramic pigments. Part 1. Crystal structure and phase transformations, Ceram. Int. 32 (4) (2006) 385–392.
[18] M. Dondi, G. Cruciani, G. Guarini, F. Matteucci, M. Raimondo, The role of counterions (Mo, Nb, Sb, W) in Cr-, Mn-, Ni- and V-doped rutile ceramic pigments. Part 2. Colour and technological properties, Ceram. Int. 32 (4) (2006) 393–405.
[19] E.C. Bucharsky, G. Schell, R. Oberacker, M.J. Hoffmann, Anatase-rutile transformation in TiO_2–V_2O_5 catalyst coatings for ceramic foams, J. Eur. Ceram. Soc. 29 (10) (2009) 1955–1961.
[20] I. Tunc, M. Bruns, H. Gliemann, M. Grunze, P. Koelsch, Bandgap determination and charge separation in Ag@TiO_2 core shell nanoparticle films, Surf. Interface Anal. 42 (6–7) (2010) 835–841.
[21] S. Shevell, The Science of Color, second ed., Elsevier, Oxford, 1979.
[22] M. Dondi, F. Matteucci, G. Baldi, A. Barzanti, G. Cruciani, I. Zama, C.L. Bianchi, Gray-blue Al_2O_3–MoO_x ceramic pigments: crystal structure, colouring mechanism and performance, Dyes Pigments 76 (1) (2008) 179–186.